

HAYABUSA2 LANDING SITE SELECTION (LSS) TRAINING: SUMMARY REPORT OF SCIENTIFIC EVALUATION. H. Yabuta¹, N. Hirata², R. Honda³, Y. Ishihara⁴, K. Kitazato², M. Komatsu⁵, A. Miura⁴, K. Matsumoto⁶, T. Morota⁷, T. Nakamura⁸, A. Nakato⁹, T. Noguchi¹⁰, T. Okada⁴, N. Sakatani¹¹, S. Sugita¹², S. Tachibana¹², S. Tanaka⁴, E. Tatsumi¹², S. Watanabe⁷, T. Yamaguchi⁴, Y. Yamamoto⁴, LSSAA Team (Hayabusa2 Project), ¹Hiroshima University, Japan (hyabuta@hiroshima-u.ac.jp), ²University of Aizu, Japan, ³Kochi University, Japan, ⁴ISAS/JAXA, Japan, ⁵Sokendai, Japan, ⁶NAOJ, Japan, ⁷Nagoya University, Japan, ⁸Tohoku University, Japan, ⁹Kyoto University, Japan, ¹⁰Kyushu University, Japan, ¹¹Meiji University, Japan, ¹²Tokyo University, Japan.

Introduction: The Japanese C-type asteroid sample return mission, Hayabusa2, was launched on December 3, 2014. The spacecraft is scheduled to arrive at a near Earth asteroid Ryugu in July 2018. During its 18-month stay, remote-sensing observations will be carried out with the on-board instruments, Optical Navigation Camera (ONC), Near Infrared Spectrometer (NIRS3), Thermal Infrared Imager (TIR), and Light Detection and Ranging (LIDAR). Hayabusa2 is planned to collect asteroid samples from up to three sites. Based on the remote-sensing data, we will carry out the landing site selection (LSS) within less than a couple of months after the arrival to Ryugu, for the first sampling touch down and for releasing MASCOT, a hopping rover developed by DLR and CNES, in October 2018.

It is therefore very important that scientists from remote sensing team, MASCOT team, and sample analyses team work together to decide a LSS strategy by sharing a common picture of the multi-scale asteroid science. During June-August 2017, we carried out an LSS training by using a polygon shape model for a Ryugu analog, “Ryugoid”.

Scientific goal of Hayabusa2 mission and Priority for LSS: The main scientific goals of Hayabusa2 are to understand (1) the origin and evolution of the solar system and (2) the formation process and structure of the asteroid [1]. Based on the mission’s scientific goals, the most scientifically valuable site for the first touch down will be a an aqueously altered region.

Overview of the asteroid Ryugoid: Data were acquired at every 90° longitude, viewing from north (Fig. 1). During this LSS observation phase soon after the arrival, the North Pole is visible from the home position (HP), and the south of 60°S is invisible. The body is in size of approximately 840±40 m in diameter. The surface is dark, but several craters exhibit high reflectance. Some regions have many craters, and other regions contain plains and boulders.

Data products used for evaluation: Six potential landing sites (zones A, B, C, D, D2, and E, in Fig. 2) were proposed based on spacecraft safety by the system engineering team. Scientific evaluations of these zones were conducted based on the data products obtained from Box A (at 20 km in altitude), Box C (at 5-7 km in altitude) and mid-altitude (at 5 km in altitude) by

Shape modeling, ONC, NIRS3, TIR, and LIDAR teams. ONC produced the six types of spectral indices (Fig. 3): (i) 0.7-μm absorption depth, (ii) space weathering index [2], (iii) spectral slope from 0.39 μm to 0.95 μm, (iv) spectral slope in ultraviolet, (v) 0.95 μm absorption depth, (vi) scores of PC1 to PC5. Boulder size-frequency measurements in the candidate landing areas were also performed. NIRS3 produced the four types of spectral feature maps: (i) 3-μm band depth (ii) 3-μm band center (iii) spectral slope, and (iv) near-infrared albedo (Fig. 4). TIR provides thermal inertia maps, typical grain size maps, and maximum temperature maps at 2018-10-22, for the first touch down (TD1).

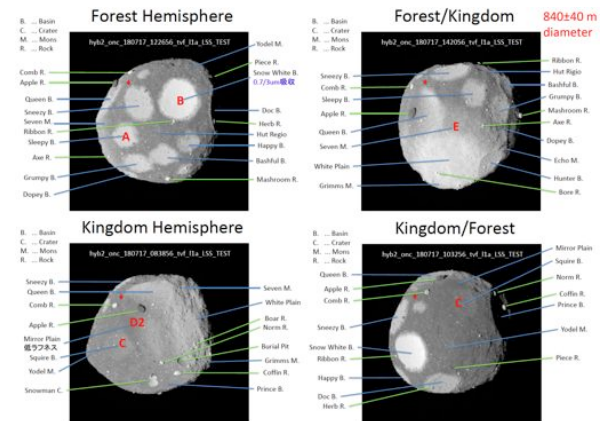


Fig. 1. The overview images of the Ryugoid.

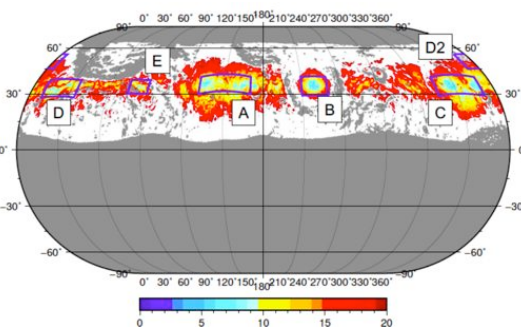


Fig. 2. The six potential landing sites (zones A-E).

Scientific evaluation for LSS: According to the 0.7-μm and 3-μm absorption features of the global maps and reflectance spectra (Figs. 3 and 4), of the six potential landing sites, the craters (zones A, B and C)

contain much more abundant hydrous minerals than the other surfaces (zones D, D2, and E). In particular, zone B with strongest absorption at $3\ \mu\text{m}$ contains the highest abundance of hydrous minerals. However, these zones are chemically different; zones A and B have an absorption peak at $\sim 2.8\ \mu\text{m}$, consistent with serpentine-type hydrous minerals, that is, CM and CR chondrites-like materials (Fig. 4). On the other hand, zone C has an absorption peak at $\sim 2.7\ \mu\text{m}$, consistent with saponite-type hydrous minerals, that is, CI-chondrite-like material (Fig. 4). Asteroid surfaces not exposed with craters are poor in hydrous minerals. These are zones D, D2, and E and may have experienced thermal metamorphism-induced dehydration, e.g., solar radiation heating.

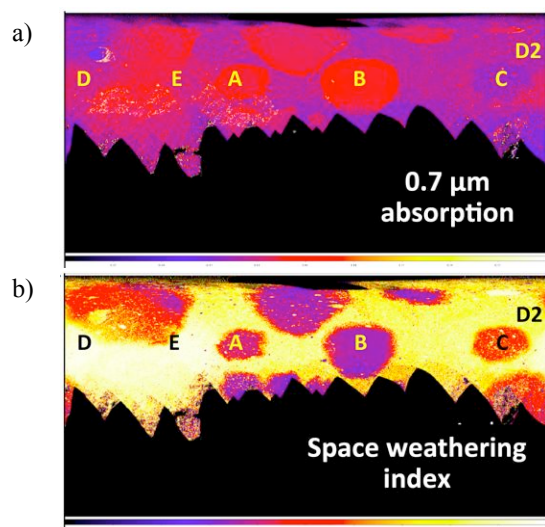


Fig. 3. Map data of a) $0.7\text{-}\mu\text{m}$ absorption and b) space weathering index acquired through the mid-altitude observation by ONC.

Since space weathering depletes hydrous minerals, regions with low space weathering index are higher priority for landing. The ranking of space weathering index can be estimated in order of increasing; $B < A < C < D \sim E$. According to the 0.39- and $0.55\text{-}\mu\text{m}$ reflectance, the order of insoluble organic matter (IOM) contents can be estimated as; $D2 \sim C (2\%) > D \sim E > A > B (1\%)$. The order of total carbon contents can be estimated as; $D2 \sim C (5\%) > A \sim B (2\%) \sim D \sim E$.

In order to evaluate the safety and a recovery rate of sampling, boulder size-frequency is important information. In this regard, the region with fewer boulders is more desirable. Based on the number of boulders (diameter $> 30\ \text{cm}$) per a circular region of $50\ \text{m}$ radius, the order of priority is; $B (< 310) > D2 (1850) > E (11000) \sim D (19000) \sim C (23000) \sim A (30000)$.

According to the map data of thermal inertia obtained by TIR (Fig. 5), maximum temperature is homo-

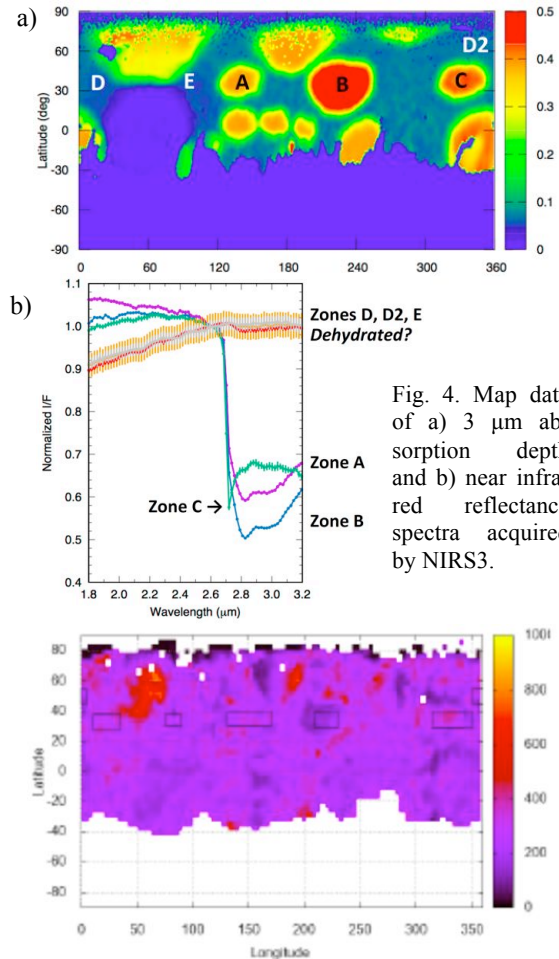


Fig. 4. Map data of a) $3\ \mu\text{m}$ absorption depth and b) near infrared reflectance spectra acquired by NIRS3.

Fig. 5. Map data of thermal inertia acquired through the mid-altitude observation by TIR.

geneously $375\text{--}380\text{K}$. Grain sizes in all the regions are at the level of several mm. Zone B ($2.8 \pm 1.5\ \text{mm}$) is regarded as the highest priority and zone D2 ($4.3 \pm 3.4\ \text{mm}$) as the second highest priority for landing.

Total evaluation and summary: Summarizing the chemical and geological characteristics of the zones A, B, C, D, D2 and E, we selected the regions that meets both the scientific value and safety for TD1. We concluded that the highest priority candidate for the TD1 site is zone B, and the second candidate is zone D2.

Through the LSS training, we have acquired the procedures to find an aqueously altered region for TD1 of Ryugu. These procedures are not only essential for LSS but also extremely useful for understanding the formation scenario of the asteroid, such as global process of aqueous alteration, dehydration, formation age of asteroid surface, by combination of sample analyses.

References: [1] Tachibana. S. et al. (2014) *Geochemical Journal* 48, 571-587. [2] Hiroi T. et al. (2011) *LPS XLII*, Abstract #1264.